

## Distorted wave analysis of the $^{17}\text{O}(t,p)^{19}\text{O}$ reaction\*

D. J. Crozier,† H. T. Fortune, and R. Middleton

*Physics Department, University of Pennsylvania, Philadelphia, Pennsylvania 19174*

J. L. Wiza

*Department of Physics, St. Joseph's College, Philadelphia, Pennsylvania 19104*

(Received 30 October 1974)

The angular distributions of  $^{17}\text{O}(t,p)^{19}\text{O}$  transitions to 13 states in  $^{19}\text{O}$  have been analyzed by distorted wave techniques. Two-particle transfer amplitudes from recent ( $sd$ )<sup>3</sup> shell-model calculations have been utilized to aid in the interpretation of the structure of  $^{19}\text{O}$ . The theoretical calculations reproduce the  $L$  admixtures in the angular distributions remarkably well for many of the low-lying states. Ratios of measured-to-predicted cross sections are consistent to within a factor of 3. The correspondence between the experimentally known states of  $^{19}\text{O}$  and those predicted by the shell-model calculations is discussed; most of the states with known  $J^\pi$  are well accounted for.

[ NUCLEAR REACTIONS  $^{17}\text{O}(t,p)$ :  $E=12.0$  MeV, DWBA analysis of old data using shell-model wave functions. ]

### I. INTRODUCTION

In recent years, an increasing amount of both theoretical and experimental interest has been shown in the region of the Periodic Table commonly known as the  $sd$  shell. The nuclei between  $^{16}\text{O}$  and  $^{40}\text{Ca}$ , which comprise the  $2s-1d$  shell, are systems of intermediate complexity. While these nuclei in general present larger numbers of states and more complicated level schemes for study than do the lighter nuclei, they do not (as do many heavier nuclei) possess such high level densities as to make experimental study prohibitively difficult, nor is their structure so complex as to make interpretation improbable. The lower part of the  $sd$  shell has, in fact, been treated quite successfully with sophisticated shell-model calculations.<sup>1,2</sup>

Among the light  $s-d$  shell nuclei, the structure of  $^{19}\text{O}$  is expected to have one of the simplest interpretations. For most of the low-lying positive-parity states, it is convenient to think of this nucleus as three neutrons outside of an  $^{16}\text{O}$  core. Since  $^{16}\text{O}$  is a reasonably good closed-shell nucleus, the structure of many of the low-lying states is dominated by  $(sd)^3$  configurations. Although the expected simplicity of the structure of  $^{19}\text{O}$  makes it an appealing nucleus to investigate, it is unfortunately, rather difficult to study experimentally. In fact,  $^{19}\text{O}$  can be produced conveniently only by means of the  $^{18}\text{O}(d,p)^{19}\text{O}$  and  $^{17}\text{O}(t,p)^{19}\text{O}$  reactions. It is therefore very useful to reanalyze data from the  $^{17}\text{O}(t,p)^{19}\text{O}$  reaction in the light of distorted-wave techniques and shell-

model computations. Although the experimental data discussed in the present paper had been published previously,<sup>3</sup> it had been analyzed only with plane wave theory.

Two-particle-transfer reactions have become an increasingly important tool in nuclear spectroscopy. Although these reactions may populate a larger set of states than do the single-particle-transfer reactions, they nevertheless obey important selection rules. In particular, in the  $(t,p)$  reaction the isospin transfer is limited to the value  $T=1$  and the spin transfer to the value  $S=0$ . Thus the total angular momentum transfer  $J$  is equal to the orbital angular momentum transfer  $L$ . In the case under present consideration, the  $^{17}\text{O}(t,p)^{19}\text{O}$  reaction, the spin of the target nucleus is  $\frac{5}{2}$ . This means that the transitions to most of the states in the residual nucleus will be characterized by mixtures of more than one  $L$  value. Hence, the shapes of the angular distributions, as well as the absolute values of the cross sections, will be configuration dependent. The  $^{17}\text{O}(t,p)^{19}\text{O}$  reaction should thus provide a sensitive test of shell-model calculations.

The recent experimental interest in the lower part of the  $sd$  shell has been accompanied and partially motivated by the advent of sophisticated shell-model calculations<sup>1,2</sup> for this region of the Periodic Table. These calculations have been successful in reproducing the properties—such as excitation energies, magnetic moments, electric quadrupole moments,  $B(E2)$  strengths and particularly spectroscopic strengths for single-nucleon transfer—of the nuclei in this region.

TABLE I. Results of shell-model calculations (Ref. 2).

Shell-model state		$L$	Two-nucleon transfer amplitudes					
$E_x$	$J^\pi$		$(d_{5/2})^2$	$(s_{1/2})^2$	$(d_{3/2})^2$	$d_{5/2}, s_{1/2}$	$d_{5/2}, d_{3/2}$	$s_{1/2}, d_{3/2}$
1.53	$\frac{1}{2}_1^+$	2			0.0343	-0.8764	0.0279	-0.1256
6.56	$\frac{1}{2}_2^+$	2			-0.2130	-0.0356	-0.8747	0.5667
0.06	$\frac{3}{2}_1^+$	2	-1.2273		-0.1015	0.5635	0.0498	0.1777
		4	0.7762				0.1168	
3.09	$\frac{3}{2}_2^+$	2	0.7220		-0.0158	0.9702	-0.0758	0.0954
		4	-0.4566				-0.1764	
5.20	$\frac{3}{2}_3^+$	2	-0.1919		-0.0634	-0.0807	-0.5145	0.2029
		4	0.1214				-0.8416	
0.00	$\frac{5}{2}_1^+$	0	-0.7312	-0.3354	-0.2181			
		2	0.8175		0.0342	-0.0453	-0.0952	-0.0769
		4	1.0968				0.1554	
2.99	$\frac{5}{2}_2^+$	0	0.1459	-0.6511	0.0001			
		2	-0.1629		-0.0561	0.5006	-0.0630	0.1682
		4	-0.2186				0.0044	
4.57	$\frac{5}{2}_3^+$	0	0.2152	-0.6718	0.0359			
		2	-0.2406		0.0389	-0.4554	-0.0630	0.1682
		4	-0.3228				0.0044	
6.91	$\frac{5}{2}_4^+$	0	-0.1478	0.0766	-0.1197			
		2	0.1652		0.0996	0.1066	0.7621	0.0559
		4	0.2217				-0.8925	
3.05	$\frac{7}{2}_1^+$	2			-0.1072	+1.2410	-0.0898	+0.1767
		4					-0.0881	
6.28	$\frac{7}{2}_2^+$	2			-0.0706	-0.1090	-0.5938	0.2727
		4					-0.9804	
2.56	$\frac{9}{2}_1^+$	2	0.7430		0.0461	-0.0686	0.2102	-0.1628
		4	-1.4227				-0.2329	
5.28	$\frac{9}{2}_2^+$	2	-0.1799		0.0225	-0.3653	-0.0151	-0.3849
		4	0.3445				0.0168	

The two-particle-transfer reactions serve as an even more refined test of the shell-model wave functions.

## II. ANALYSIS AND RESULTS

The results of the shell-model calculation<sup>2</sup> that are pertinent to the analysis of the  $^{17}\text{O}(t, p)^{16}\text{O}$  reaction are given in Table I. The first two columns of this table identify the states by means of the predicted excitation energies and spin-parity values. The third column lists the allowed angular momentum transfers  $L$  for the transitions to each state. The last six columns of the table

give the shell-model results<sup>2</sup> for the two-nucleon-transfer amplitudes, as defined, e.g. by Glendenning.<sup>4</sup>

The optical-model parameters used in the distorted-wave Born-approximation (DWBA) calculations are given in Table II. Because of the lack of available triton elastic scattering data, parameters determined for  $^3\text{He}$  were used for the entrance channel.<sup>5</sup> For the exit channel the global proton parameter set determined by Watson, Singh, and Segel<sup>6</sup> was used. The DWBA calculations were performed using the two-particle-transfer option in the code DWUCK<sup>7</sup>.

TABLE II. Optical-model parameters used in distorted-wave calculations.

	$V$ (MeV)	$r_0$ (fm)	$a$ (fm)	$W$ (MeV)	$W' = 4W_D$ (MeV)	$r'_0$ (fm)	$a'$ (fm)	$V_{so}$ (MeV)	$r_{so}$ (fm)	$a_{so}$ (fm)	$r_{Coul}$ (fm)
$t^a$	177	1.138	0.724	12	0	1.60	0.769	5	1.138	0.724	1.40
$p^b$	$V(p)^c$	$r(p)^d$	0.57	0	$W'(p)^e$	$r(p)^d$	0.5	5.5	$r(p)^d$	0.57	$r(p)^d$

<sup>a</sup> H. T. Fortune *et al.*, Phys. Rev. **185**, 1548 (1969).

<sup>b</sup> B. A. Watson *et al.*, Phys. Rev. **182**, 977 (1968).

<sup>c</sup>  $V(p) = 60 + 0.04(Z/A^{1/3}) + 27(N-Z)/A - 0.3E$ .

<sup>d</sup>  $r(p) = 1.15 - 0.001E$ .

<sup>e</sup>  $W'(p) = 4 \times \begin{cases} 10(N-Z)/A + 0.64E, & \text{for } E < 13.8 \\ 10(N-Z)/A + 9.6 - 0.06E, & \text{for } E \geq 13.8. \end{cases}$

The angular distributions from the  $^{17}\text{O}(t, p)^{19}\text{O}$  reaction are compared with the DWBA predictions in Figs. 1–3. Figure 1 contains the states with reasonably certain shell-model counterparts. The solid lines in Fig. 1 represent the theoretical

cross sections independently normalized for each level but calculated with the transfer amplitudes of Table I. The broken lines represent the contribution to the theoretical cross section from each possible  $L$  value component. The contribu-

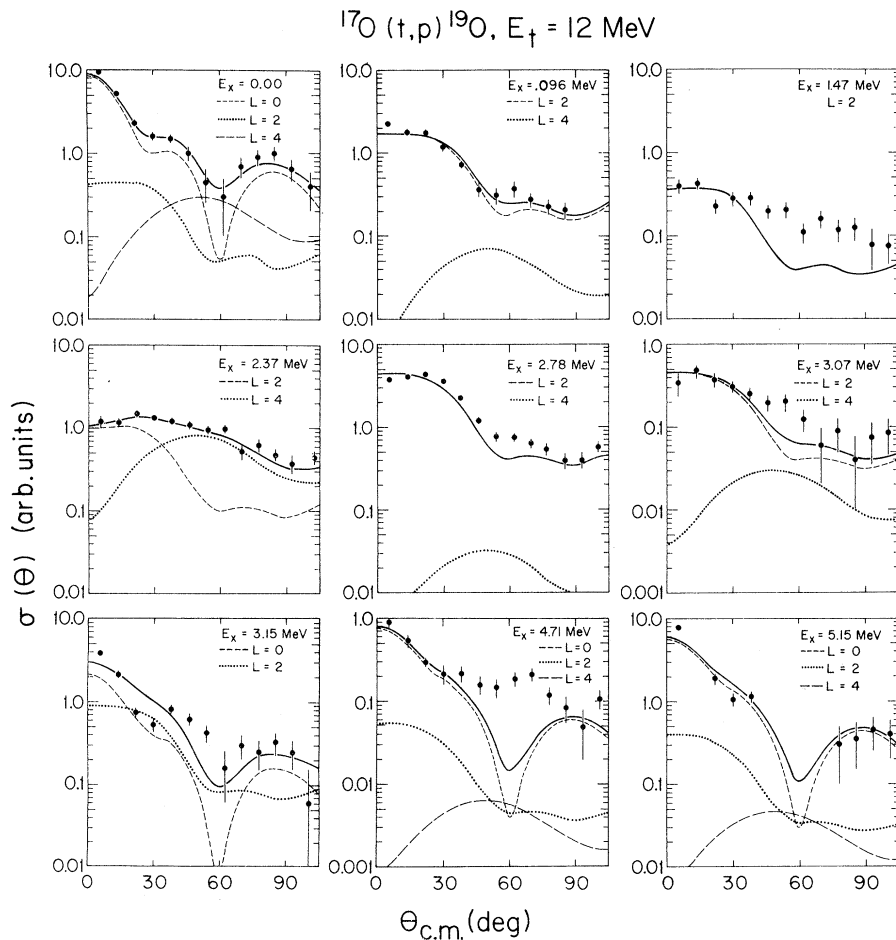


FIG. 1. Angular distributions of the  $^{17}\text{O}(t, p)^{19}\text{O}$  reaction for states with reasonably good shell-model counterparts. The curves are results of DWBA calculations using transfer amplitudes from Table I. The  $L$  admixtures are as predicted by those amplitudes, but over-all magnitude has been adjusted independently for each level, giving ratios listed in Table III.

tion from different  $L$  values is that given by the shell-model calculations. The angular distributions in Figs. 2 and 3 have been fitted with arbitrary admixtures of the various  $L$  values. These components are represented by the broken lines, while the solid lines represent their sum.

The relative normalizations ( $N = \sigma_{\text{exp}}/\sigma_{\text{th}}$ ) for the experimental states that have been identified with specific shell-model states are given in Table III. Here, the experimental states are identified by excitation energy and spin-parity<sup>8</sup> in the first two columns of the table. The theoretical identifications given in the third and fourth columns are the same as those listed in Table I. Since the authors of Ref. 3 measured only relative cross sections, the absolute values of these ratios are not known. The over-all magnitude of the relative normalizations shown in the last column of Table III has been adjusted so that the average of the normalizations for the first six states in  $^{19}\text{O}$ —those for which shell model counterparts may be firmly established—is equal to 100. For convenience in discussing individual states, we include in Table IV both the excitation energies from the  $(t, p)$  data<sup>3</sup> and those from a recent compilation.<sup>8</sup> The most recent spin-parity assignments, including the results of the present work, are also presented in Table IV.

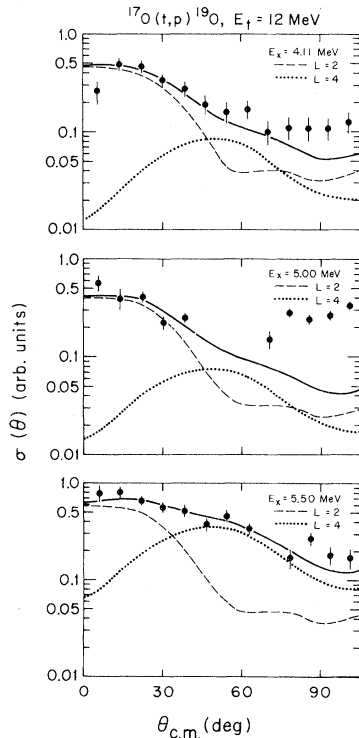


FIG. 2. Angular distributions for probable  $(sd)^3$  states at 4.11, 5.00, and 5.50 MeV, with arbitrary admixtures of  $L=2$  and 4 DWBA curves.

### III. DISCUSSION

We discuss first those states that can be most reliably identified with specific shell-model states. We then discuss the other states at low excitation energy—those which have no obvious counterpart in the present shell-model calculations and/or which were not observed in the  $^{17}\text{O}(t, p)^{19}\text{O}$  reaction.

#### A. States at 0.00, 0.096, and 1.47 MeV excitation

The angular distributions for the transitions to these three states are shown at the top of Fig. 1. The identification of these three states with specific shell-model states is well established.

An  $L=0$  component observed in the  $^{17}\text{O}(t, p)^{19}\text{O}$  angular distribution for the ground state led<sup>3,9</sup> to the assignment  $J^\pi = \frac{5}{2}^+$ . This state is strongly populated by an  $l_n=2$  transition in the  $^{18}\text{O}(d, p)^{19}\text{O}$  reaction.<sup>3, 10-14</sup>  $\gamma$ -decay data also give a  $J = \frac{5}{2}$  assignment.<sup>15</sup> The shell-model counterpart of the ground state is, of course,  $\frac{5}{2}^+$ . As can be seen in Fig. 1, the present DWBA calculation reproduces the shape of the ground state (g.s.) angular distribution, a mixture of  $L=0, 2$ , and 4 components, extremely well. That the normalization  $N$ , given in Table III, for the ground state is larger than that for the other levels is probably

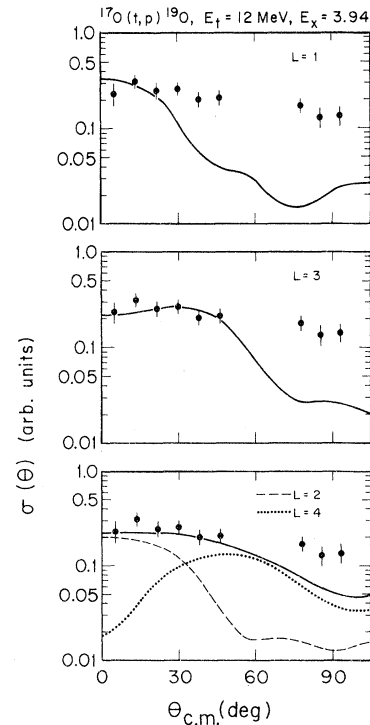


FIG. 3. Angular distribution for the 3.945-MeV state, together with  $L=1, 2, 3$ , and 4 DWBA curves.

TABLE III. Relative normalizations of experimental and theoretical cross sections.

Experimental state		Theoretical state		Relative normalization $N = \sigma_{\text{exp}}/\sigma_{\text{th}}^a$
$E_x$ (MeV)	$J^\pi$	$E_x$ (MeV)	$J^\pi$	
0.00	$\frac{5}{2}^+$	0.00	$\frac{5}{2}_1^+$	180
0.10	$\frac{3}{2}^+$	0.06	$\frac{3}{2}_1^+$	107
1.47	$\frac{1}{2}^+$	1.53	$\frac{1}{2}_1^+$	68
2.373	$\frac{9}{2}^+$	2.56	$\frac{9}{2}_1^+$	112
2.78	$\frac{7}{2}^+$	3.05	$\frac{7}{2}_1^+$	74
3.07	$\frac{3}{2}^+$	3.09	$\frac{3}{2}_2^+$	59
3.15	$\frac{5}{2}^+$	2.99	$\frac{5}{2}_2^+$	101
4.71	$\frac{5}{2}^+$	4.57	$\frac{5}{2}_3^+$	42
5.15	$\frac{5}{2}^+$	4.57	$\frac{5}{2}_3^+$	68

<sup>a</sup> $N_{\text{average}} = 100$  for first six states.

caused by coherence phenomena. Shell-model calculations frequently underestimate the amount of coherence in ground states.

The  $^{18}\text{O}(d, p)^{19}\text{O}$  reaction populates the 0.096-MeV state by a very weak  $l_n=2$  transition (about  $\frac{1}{30}$  of the g.s.<sup>3, 10, 11, 16</sup>). This assigns positive parity as does the  $L=2$  distribution produced by the  $^{17}\text{O}(t, p)^{19}\text{O}$  reaction.<sup>3, 9</sup> The  $\gamma$  cascade of the 1.46-MeV state assigns<sup>15</sup>  $J = \frac{3}{2}$  to the 0.096-MeV level. Thus  $J^\pi = \frac{3}{2}^+$ . The shell model produces a low-lying  $\frac{3}{2}^+$  state, essentially degenerate with the ground state. The predicted angular distribution for this state is compared with the experimental angular distribution in Fig. 1. The predominantly  $L=2$  character of the angular distribution is predicted by the calculation, and the normalization  $N$  is close to the mean obtained for the other low-lying states.

A strong  $l_n=0$  angular distribution observed in the  $^{18}\text{O}(d, p)^{19}\text{O}$ <sup>3, 16</sup> reaction assigns  $\frac{1}{2}^+$  to the 1.46-MeV state. This level decays predominately to the 0.096-MeV<sup>17-19</sup> state with only a weak branch to the ground state. The second excited state in the shell-model calculations has  $J^\pi = \frac{1}{2}^+$ , though its exact position is highly sensitive to the details of the calculation. In Fig. 1, the theoretical calculation for this state fits the experimental distribution less well than for the lower levels, and the resulting normalization is somewhat below the average. However, the cross section for this state is so small that processes other than direct one-step  $2n$  transfer may be important.

TABLE IV. Excitation energies and spin assignments in  $^{19}\text{O}$ .

$E_x$ (MeV $\pm$ keV)		$J^\pi$ <sup>c</sup>
$(t, p)$ <sup>a</sup>	Literature <sup>b</sup>	
0.000	0.000	$\frac{5}{2}^+$
0.096	$0.0960 \pm 0.5$	$\frac{3}{2}^+$
1.471	$1.4717 \pm 0.4$	$\frac{1}{2}^+$
2.373	$2.3711 \pm 1.0$	$\frac{9}{2}^+$
2.779	$2.7787 \pm 0.8$	$\frac{7}{2}^+$
3.070	$3.0671 \pm 2.6$	$\frac{3}{2}^+$
3.157	$3.1545 \pm 2.0$	$\frac{5}{2}^+$
	$3.235 \pm 4$	$\frac{3}{2}^+$
3.946	$3.9453 \pm 2.5$	$\frac{3}{2}^-$
4.111	$4.116 \pm 4$	$\frac{3}{2}^+$
(4.337)	$4.333 \pm 12$	
(4.402)	$4.400 \pm 9$	
	$4.583 \pm 8$	$\frac{3}{2}^-$
4.706	$4.707 \pm 12$	$\frac{5}{2}^+$
4.998	$4.998 \pm 12$	
	$5.086 \pm 10$	$\frac{1}{2}^-$
5.154	$5.149 \pm 7$	$\frac{5}{2}^+$
	$5.455 \pm 9$	$\frac{3}{2}^+$
5.502	$5.502 \pm 12$	
	5.53	$(\frac{1}{2}^-)$
	$5.706 \pm 8$	$(\frac{3}{2}^+)$

<sup>a</sup> Reference 3.

<sup>b</sup> Reference 7.

<sup>c</sup> Including results of the present work.

#### B. States at 2.37, 2.78, and 3.07 MeV excitation

The analysis of the  $^{17}\text{O}(t, p)^{19}\text{O}$  reaction populating these three states has recently been discussed in detail.<sup>20</sup> Here we shall mention only that, on the basis of the present work and recent  $\gamma$ -decay studies,<sup>18, 19</sup> assignments of  $J^\pi = \frac{9}{2}^+$  for the 2.37-MeV,  $\frac{7}{2}^+$  for the 2.78-MeV, and  $(\frac{3}{2}^+)$  for the 3.07-MeV level have been made. For completeness the angular distributions for these three states are shown in the middle of Fig. 1, and the normalizations are given in Table III.

#### C. States at 3.15, 4.71, and 5.15 MeV excitation

The angular distributions of these three states are shown in the bottom of Fig. 1. All three of these distributions exhibit an  $L=0$  component, and hence they all were assigned<sup>3, 9</sup>  $J^\pi = \frac{5}{2}^+$ .

The level at 3.15 MeV is populated by a  $l_n=2$

transition in the  $^{18}\text{O}(d,p)^{19}\text{O}$  reaction.<sup>3,11,16</sup> A study of the  $^{18}\text{O}(\bar{d},p)^{19}\text{O}$  reaction<sup>21</sup> requires  $J^\pi = \frac{5}{2}^+$ , though the fit to the cross section is not perfect at forward angles. The  $\gamma$  decay is predominantly to the  $\frac{1}{2}^+$  level at 1.47 MeV. The  $(t,p)$  angular distribution for this state is shown in Fig. 2 together with the theoretical calculation for the  $\frac{5}{2}^+$  level. Although the normalization is close to the average value, the fit is poorer than for the states previously discussed. Therefore, we hesitate to conclude that this state corresponds closely to the  $(\frac{5}{2})_2^+$  theoretical state. Of course, the poor fit may simply be due to an inability of the DWBA calculations to fit the  $Q$  dependence of  $L=0$  shapes.

The 4.71-MeV state has been assigned  $\frac{5}{2}^+$  because of the  $L=0$  component in its  $^{17}\text{O}(t,p)^{19}\text{O}$ <sup>3</sup> angular distribution. Its angular distribution is shown in Fig. 1, with the theoretical distribution for the third theoretical  $\frac{5}{2}^+$  state. As can be seen, the fit is imperfect; a larger  $L=4$  component would seem to be required in order to fit the data. In addition, the normalization is smaller than the average by more than a factor of 2. We return to this point below.

The  $\frac{5}{2}^+$  assignment for the 5.15-MeV state comes from the  $L=0$  component in the  $^{17}\text{O}(t,p)^{19}\text{O}$  angular distribution.<sup>3</sup> An assignment<sup>22</sup> of  $J = \frac{3}{2}$  from peak-height analysis of neutron scattering contradicts this assignment. However, the reliability of that technique for this state is questionable, since the measured width of  $3.6 \pm 1.0$  keV is comparable to the experimental resolution of 2.5 keV. Also, recent measurements<sup>21</sup> of the vector analyzing power (VAP) in the  $^{18}\text{O}(\bar{d},p)^{19}\text{O}$  reaction require  $J^\pi = \frac{5}{2}^+$  for this state. In Fig. 1, the experimental  $(t,p)$  angular distribution for the 5.15-MeV state is compared with the theoretical calculation for the third  $\frac{5}{2}^+$  shell-model level. As can be seen, the fit is reasonably good, but data were not extracted at a number of angles. Since the angles having missing data are near the  $L=4$  peak, the  $L=4$  component may be much larger than shown for this level. We note also that the normalization, in Table III, is considerably smaller than average. Thus, both the 4.71- and 5.15-MeV states are weaker than the third  $\frac{5}{2}^+$  state should be. However, the sum of their cross sections is close to that expected for the third  $\frac{5}{2}^+$  state. This suggests that these two states share the strength of the  $(\frac{5}{2})_3^+$  state, presumably because the  $(sd)^3$  state has mixed with a  $\frac{5}{2}^+$  state not contained in the present shell-model calculation. The fourth  $\frac{5}{2}^+$  shell-model state would then presumably lie higher in excitation.

However, the theoretical angular distribution (not shown) for the fourth  $\frac{5}{2}^+$  shell-model state is

predicted to be nearly pure  $L=4$ . Thus the possibility also exists that the 4.71- and 5.15-MeV states share the strength of the third and fourth  $\frac{5}{2}^+$  shell-model states, but in a manner different from that of the calculations. The fourth  $\frac{5}{2}^+$  model state would then provide the additional  $L=4$  strength that seems to be required for the 4.71-MeV state and cannot be ruled out for the 5.15-MeV state.

#### D. States at 4.11, 5.00, and 5.50 MeV excitation

Three angular distributions are shown in Fig. 2, fitted by arbitrary admixtures of  $L=2$  and 4 components. That these data can be well fitted with admixed  $L=2$  and 4 distributions suggests that the structure of the corresponding states is  $(sd)^3$ . However, it is premature to assign shell-model counterparts to them.

The angular distribution<sup>3</sup> of the 4.11-MeV state in the  $^{18}\text{O}(d,p)^{19}\text{O}$  reaction lies between the expected shapes for  $l=1$  and  $l=2$ . However, the  $^{17}\text{O}(t,p)^{19}\text{O}$  angular distribution was taken as evidence<sup>3</sup> for positive parity. It is fitted best by a mixture of  $L=2$  and 4; thus the  $J^\pi$  for this state is restricted to  $(\frac{3}{2} - \frac{9}{2})^+$ . Previously, the 4.11-MeV state had a tentative  $J^\pi$  assignment<sup>9</sup> of  $(\frac{3}{2}, \frac{5}{2})^+$ . The VAP measurements in  $^{18}\text{O}(\bar{d},p)^{19}\text{O}$  require<sup>21</sup>  $J^\pi = \frac{3}{2}^+$ . This state is then probably to be identified with the third  $\frac{3}{2}^+$  shell-model state.

The angular distribution of the 5.00-MeV state has also been fitted in Fig. 2 with an  $L=2$  and 4 mixture. This would imply the assignment  $J^\pi = (\frac{3}{2}^+ - \frac{9}{2}^+)$ , but the poor quality of the fit weakens the assignment. A state previously known at 4.998 MeV has no suggested spin-parity assignment. Results of the  $^{13}\text{C}(^7\text{Li},p)^{19}\text{O}$  reaction<sup>23</sup> suggest a high spin ( $\geq \frac{7}{2}$ ). No shell-model counterpart can be suggested.

The angular distribution for the 5.50-MeV level is well fitted by an  $L=2$  and 4 mixture. This combination of  $L$  values assigns  $J^\pi = (\frac{3}{2} - \frac{9}{2})^+$ . This state is not observed in the  $^{18}\text{O}(d,p)^{19}\text{O}$  reaction,<sup>3</sup> but may be obscured in that reaction by the strong, broad  $\frac{3}{2}^+$  state at 5.46 MeV. In the shell-model scheme, this state can be most conveniently associated with the  $\frac{7}{2}^+$  level. However, this correspondence is based solely upon the excitation energy, and present limits on  $J^\pi$ .

#### E. 3.95-MeV state

The only level not so far discussed for which an angular distribution has been extracted is the 3.945-MeV state. A state at this energy was populated with  $l_n=1$  in the  $^{18}\text{O}(d,p)^{19}\text{O}$  reaction,<sup>3</sup> and has been assigned<sup>21</sup>  $J^\pi = \frac{3}{2}^-$  from the same reaction with polarized deuterons. However, the  $^{13}\text{C}(^7\text{Li},p)-$

$^{19}\text{O}$  reaction<sup>23</sup> indicates that the 3.95-MeV "level" is actually a doublet, with one member having high spin. We do not know, *a priori*, which of the two states is being excited in the  $^{17}\text{O}(t, p)^{19}\text{O}$  reaction. If it is the  $\frac{3}{2}^-$  member that is being excited, then this is the only negative-parity state below 6 MeV that has any observable  $(t, p)$  strength. Since the low-lying negative-parity states are likely due to  $1p$ -shell holes, their nonobservation in  $(t, p)$  is to be expected. The 3.95-MeV level has a characteristic  $l=1$  angular distribution in  $(d, p)$ ,<sup>3, 21</sup> but a small spectroscopic factor<sup>3, 21</sup> ( $S \sim 0.1$ ). The  $(t, p)$  cross section for the 3.95-MeV level is the smallest of those for which angular distributions were measured. So its strength does not rule out the possibility that it is the  $\frac{3}{2}^-$  member of the doublet that is being excited. If indeed it is, then the angular distribution should be characteristic of  $L=1$  or  $L=3$  or both. The experimental angular distribution, which is reasonably flat, is compared with  $L=1$  and  $3$  DWBA curves in the top and middle of Fig. 3. The  $L=3$  curve gives a reasonable fit, but so does an admixture of  $L=2$  and  $4$ , as depicted in the bottom of Fig. 3. Thus, the shape of the angular distribution does not allow us to decide which member of the doublet is being populated in  $(t, p)$ . This state clearly deserves further study.

#### F. Other low-lying states

Of the states that are known in  $^{19}\text{O}$  below 6 MeV in excitation, several had no measurable strength in the  $^{17}\text{O}(t, p)^{19}\text{O}$  reaction. These are states at excitation energies of 3.23, 4.33, 4.58, 5.09, 5.46, 5.53, and 5.71 MeV. The state at 4.40 MeV had a cross section comparable to that of the 4.11-MeV level, but no angular distribution is available. Of these states, the ones at 4.58 and 5.09 MeV are known<sup>8</sup> to have negative parity  $\frac{3}{2}^-$  and  $\frac{1}{2}^-$ , respectively. The 5.53-MeV state has a probable ( $\frac{1}{2}^-$ ) assignment.<sup>24</sup> The 5.46-MeV state is dominantly the  $d_{3/2}$  single-particle state.<sup>21, 25</sup> Its nonobservation is due both to its large width and to the relatively small cross section expected for the  $d_{3/2}$  single-particle state in the  $^{17}\text{O}(t, p)$  reaction.

Two of the other states are also probably  $\frac{3}{2}^+$  states. The state at 3.23 MeV was suggested to have  $J = \frac{3}{2}$  from an earlier  $^{13}\text{C}(^7\text{Li}, p)^{19}\text{O}$  study,<sup>26</sup> and was populated in the  $^{18}\text{O}(d, p)^{19}\text{O}$  reaction<sup>16</sup> with a weak  $l_n=2$  angular distribution. The state at 5.71 MeV has been assigned  $J = \frac{3}{2}$  from neutron scattering.<sup>22</sup> If this  $J$  assignment is correct, and if only one level is present, then the  $^{18}\text{O}(d, p)^{19}\text{O}$  reaction<sup>21</sup> requires  $J^\pi = \frac{3}{2}^+$ . However, there is

some evidence<sup>23</sup> that this state is a doublet. The 3.23-MeV state is likely a core-excited state. (The  $0^+$  state at 3.63 MeV in  $^{18}\text{O}$  is dominantly a core-excited state,<sup>27</sup> so 3.23 MeV is not too low for such configurations to be important in  $^{19}\text{O}$ .) The lowest expected positive-parity core-excited state is a  $5p-2h \frac{3}{2}^+$  state [ $^{21}\text{Ne}(\text{g.s.}) \times ^{14}\text{C}(\text{g.s.})$ ]. Such a state should not be appreciably excited in  $^{17}\text{O}(t, p)^{19}\text{O}$ . Little is known about the 4.33- and 4.40-MeV states. They have no suggested spin assignments except from  $^{13}\text{C}(^7\text{Li}, p)^{19}\text{O}$ , which suggests<sup>23</sup> high spin. Their small cross sections in  $^{17}\text{O}(t, p)^{19}\text{O}$  might argue for negative parity. Both states are also extremely weak in  $^{18}\text{O}(d, p)^{19}\text{O}$ .

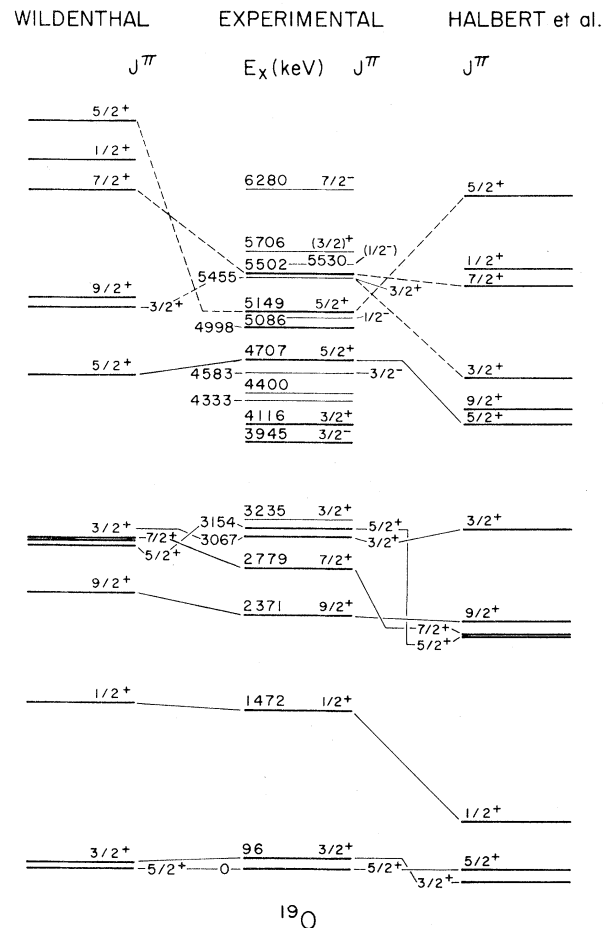


FIG. 4. Comparison of experimental and theoretical level schemes. Known levels of  $^{19}\text{O}$  are shown in the center; heavy lines denote states observed in  $^{17}\text{O}(t, p)^{19}\text{O}$ ; lighter lines, other states. Shell-model calculations used in the analysis are shown on the left, similar calculations on the right. Solid lines denote firm correspondences between theory and experiment; broken lines, the more tenuous ones.

## IV. CONCLUSIONS

The similarities of the experimental level scheme of  $^{19}\text{O}$  to the shell-model calculations of Wildenthal,<sup>2</sup> which we have been discussing, and to a similar calculation by Halbert *et al.*<sup>1</sup> are shown in Fig. 4. The experimental levels which are most strongly populated in the  $^{17}\text{O}(t,p)^{19}\text{O}$  reaction are indicated by heavy lines, other known levels by lighter lines. As we have previously observed, the lowest six levels in  $^{19}\text{O}$  have well established shell-model counterparts— $\frac{5}{2}^+$  for the ground state,  $\frac{3}{2}^+$  for the 0.10-,  $\frac{1}{2}^+$  for the 1.47-,  $\frac{3}{2}^+$  for the 2.37-,  $\frac{7}{2}^+$  for the 2.78-, and  $\frac{3}{2}^+$  for the 3.07-MeV states. In addition, a strong but less definite correspondence exists between the  $5/2^+$ <sub>2</sub> shell-model state and the 3.16-MeV experimental level. Furthermore, the 4.71- and 5.15-MeV states may be linear combinations of the  $5/2^+$ <sub>3</sub> and  $5/2^+$ <sub>4</sub> shell-model states, although they cannot be identified with these states individually. The 5.46-MeV level is dominantly the  $d_{3/2}$  single-particle state. Finally, the 4.11-, 5.00-, and 5.50-MeV states

may correspond to the  $3/2^+$ <sub>3</sub>,  $9/2^+$ <sub>2</sub>, and  $7/2^+$ <sub>2</sub> shell-model levels, respectively.

The remaining low-lying states—those at 3.23-, 3.95-, 4.33-, 4.40-, 4.58-, 5.53-, 5.71-, 6.13-, 6.20-, and 6.28-MeV—do not appear to have  $(sd)^3$  configurations. The 3.23-MeV  $(\frac{3}{2})^+$  state appears to be a core-excitation level. The remaining levels are either known to have negative parity or are likely to have. Thus none of these states would be expected to be described in the present shell-model picture, nor populated strongly in the present reaction.

In conclusion, most of the low-lying levels in  $^{19}\text{O}$  predicted by the shell model have been definitely identified in the observed level scheme and all have been at least tentatively identified. In a number of cases theoretical calculations have succeeded in predicting properly the shapes of distributions populated by a mixture of  $L$  values. Furthermore, the theory succeeds in predicting the relative strengths of the two-neutron-transfer reactions. Finally, the excitation energies of these states are reproduced reasonably well.

\*Work supported by the National Science Foundation.

†Present address: Department of Physics, Kansas State University, Manhattan, Kansas 66506.

<sup>1</sup>E. C. Halbert, J. B. McGrory, B. H. Wildenthal, and S. P. Pandya, in *Advances in Nuclear Physics*, edited by M. Baranger and E. Vogt (Plenum, New York, 1971), Vol. IV.

<sup>2</sup>B. H. Wildenthal, private communication.

<sup>3</sup>J. L. Wiza and R. Middleton, *Phys. Rev.* **143**, 676 (1966).

<sup>4</sup>N. K. Glendenning, *Phys. Rev.* **137**, B102 (1965).

<sup>5</sup>H. T. Fortune, N. G. Puttaswamy, and J. L. Yntema, *Phys. Rev.* **185**, 1548 (1969).

<sup>6</sup>B. A. Watson, P. P. Singh, and R. E. Segel, *Phys. Rev.* **182**, 977 (1969).

<sup>7</sup>P. D. Kunz, private communication.

<sup>8</sup>F. Ajzenberg-Selove, *Nucl. Phys.* **A190**, 1 (1972).

<sup>9</sup>R. Moreh, *Nucl. Phys.* **70**, 293 (1965).

<sup>10</sup>G. Wickenberg, S. Hjorth, N. G. E. Johansson, and B. Sjögren, *Ark. Fys.* **25**, 191 (1963).

<sup>11</sup>K. Yagi, Y. Nakajima, K. Katori, Y. Awaya, and M. Fujioka, *Nucl. Phys.* **41**, 584 (1963).

<sup>12</sup>W. Zimmerman, Jr., *Phys. Rev.* **114**, 837 (1959).

<sup>13</sup>J. C. Armstrong and K. S. Quisenberry, *Phys. Rev.* **122**, 150 (1961).

<sup>14</sup>R. Moreh and F. Daniels, *Nucl. Phys.* **74**, 403 (1965).

<sup>15</sup>J. P. Allen, A. J. Howard, and D. A. Bromley, *Nucl.*

*Phys.* **68**, 426 (1965).

<sup>16</sup>P. Fintz, F. Hibou, B. Rastegar, and A. Gallmann, *Nucl. Phys.* **A132**, 265 (1969); **A150**, 49 (1970).

<sup>17</sup>R. E. McDonald, J. A. Becker, A. D. W. Jones, and A. R. Poletti, *Phys. Rev. C* **4**, 377 (1971).

<sup>18</sup>C. Broude, U. Karfunkel, and Y. Wolfson, *Nucl. Phys.* **A161**, 241 (1971).

<sup>19</sup>F. Hibou, P. Fintz, B. Rastegar, and A. Gallmann, *Nucl. Phys.* **A171**, 603 (1971).

<sup>20</sup>D. J. Crozier, H. T. Fortune, R. Middleton, J. L. Wiza, and B. H. Wildenthal, *Phys. Lett.* **41B**, 291 (1972).

<sup>21</sup>S. Sen, S. E. Darden, H. R. Hiddleston, and W. A. Yoh, *Nucl. Phys.* **A219**, 429 (1974).

<sup>22</sup>F. J. Vaughn, H. A. Grench, W. L. Imhof, J. H. Rowland, and M. Walt, *Nucl. Phys.* **64**, 336 (1965).

<sup>23</sup>H. T. Fortune and H. G. Bingham, *Phys. Rev. C* **10**, 2174 (1974); and unpublished.

<sup>24</sup>F. R. Donoghue, A. F. Behof, and S. E. Darden, *Nucl. Phys.* **54**, 33 (1964).

<sup>25</sup>J. L. Wiza and H. T. Fortune, *Phys. Rev. C* **7**, 1267 (1973).

<sup>26</sup>J. L. Wiza, H. G. Bingham, and H. T. Fortune, *Phys. Rev. C* **7**, 2175 (1973).

<sup>27</sup>H. T. Fortune and S. C. Headley, *Phys. Lett.* **51B**, 136 (1974).